Irradiation-induced degradation in solar cell: characterization of recombination centres

2002 Semicond. Sci. Technol. 17 453

(http://iopscience.iop.org/0268-1242/17/5/308)

INSTITUTE OF PHYSICS PUBLISHING SEMICONDUCTOR SCIENCE AND TECHNOLOGY

Semicond. Sci. Technol. **17** (2002) 453–460 PII: S0268-1242(02)29679-0

Irradiation-induced degradation in solar cell: characterization of recombination centres

J C Bourgoin[1] **and M Zazoui**[2]

[1] Laboratoire des Milieux Désordonnés et Hétérogènes, Université Pierre et Marie Curie (Paris, VI), C.N.R.S (UMR 7603), Tour 22, 4 Place Jussieu, F-75252 Paris Cedex 05, France
[2] Laboratoire de Physique de la Matière Condensée, Faculté des Sciences et Techniques – Mohammedia, BP 146 Bd Hassan II – Mohammedia, Morocco

Received 15 October 2001, in final form 14 December 2001
Published 12 April 2002
Online at stacks.iop.org/SST/17/453

Abstract
Although the defects introduced by irradiation in Si and GaAs have been extensively studied, the centres giving rise to non-radiative recombination have been neither characterized nor identified. We propose here a method allowing one to fully characterize recombination centres, i.e. to obtain their electron and hole capture cross sections as well as their concentration. It is based on a correlation between data extracted from the current–voltage characteristics of a junction in dark, deep level transient spectroscopy and the variations of the short-circuit current and open voltage of solar cells versus the logarithm of the irradiation fluence. The method is applied to characterize and tentatively identify the recombination centres introduced by electron irradiation in Si, GaAs and InGaP.

1. Introduction

The degradation of solar cells in a space environment induced by energetic particles, such as protons and electrons, has been extensively studied for many years and is, at least to some extent, well mastered (for a recent review see [1]). It is well known that, for low irradiation fluences, this degradation is due to the introduction of non-radiative recombination centres. It is only for large fluences that trapping centres induce a non-negligible compensation of the free carriers and participate also in this degradation.

The degradation is generally described in terms of the variation of the short-circuit current (I_{SC}) and the open-circuit voltage (V_{OC}) versus the irradiation fluence (φ). Often the change of I_{SC}, or V_{OC}, is presented versus $\log\varphi$ because the plots $I_{SC}(\log\varphi)$ and $V_{OC}(\log\varphi)$ appear to be linear in the low fluence range which corresponds to space applications. However, no justification has been provided for this apparently surprising behaviour. Apparently, as illustrated in figure 1, these plots, normalized to the unirradiated values $I_{SC}(0)$ and $V_{OC}(0)$, decrease linearly with $\log\varphi$ and their slopes are used as a measure of the rate of degradation, without knowing the physical meaning they possess.

The aim of this paper is to demonstrate why the dependences of I_{SC} and V_{OC} versus $\log\varphi$ are linear and to derive the parameters which determine the slopes. This will allow one to know the approximations under which such behaviour happens and to find precisely the conditions in which they are valid. We shall see that in fact the slope is defined by the material itself and by the conditions of

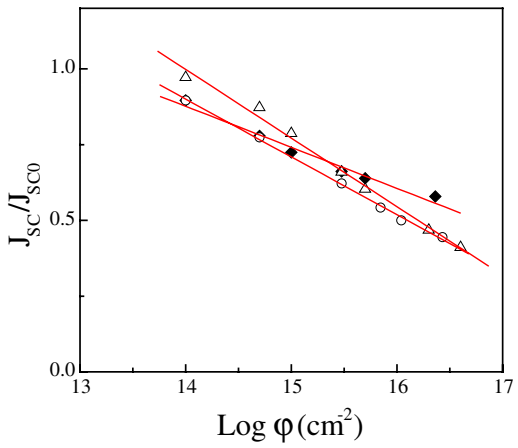

Figure 1. Variations of the short-circuit current normalized to the unirradiated value, versus fluence, for type a (♦), b (○) and c (△) Si cells. The characteristics of these cells are described in section 3.

illumination and is independent of the nature and concentration of the recombination centres. It is another characteristic parameter of the plot which gives information on these centres.

This study is substantiated by experimental data obtained using electron irradiation of Si, GaAs and GaInP solar cells. Coupled to other data, derived from deep level transient spectroscopy (DLTS) and the current–voltage characteristics of the cells in the dark, it allowed us to determine the nature, introduction rate and capture cross sections for minority carrier trapping of the non-radiative recombination centres introduced in these materials by the irradiation.

2. Mechanism of degradation

We examine, in sequence, the variations of the short-circuit current, I_{SC}, and of the open-circuit voltage, V_{OC}, induced by a fluence φ of irradiation. We recall briefly (a full treatment of solar cells can be found in [2]) that the open-circuit voltage is the voltage for which the current $I(V)$, furnished by the cell for a voltage V, difference between the generated current, I_{Ph}, and the dark current $I_{dc}(V)$

$$I(V) = I_{Ph} - I_{dc}(V) \tag{1}$$

is zero, that is

$$I_{dc}(V_{OC}) = I_{Ph}. \tag{2}$$

As to I_{Ph}, it is the short-circuit current I_{SC}

$$I_{SC} = I_{Ph} \tag{3}$$

in such way that

$$I_{dc}(V_{OC}) = I_{SC}. \tag{4}$$

2.1. Short-circuit current

The short-circuit current density J_{SC} is the sum of a generation current induced by electron–hole pair creation and of a diffusion current of electrons and holes on each side of the junction. The irradiation introduces non-radiative recombination centres which decrease the minority carrier lifetime affecting only the diffusion current. Indeed, in the short-circuit regime, the potentials are equal on both sides of the space charge region and the carrier distributions are near the equilibrium ones. The resulting rate of Shockley–Read recombination is very weak and the generation current can be considered as constant until the width of the space charge region W varies as a result of the compensation of the free carriers.

Hence, the degradation of J_{SC} is that of the diffusion current density J_d. We have therefore to examine the dependence of J_d versus the fluence φ. When the width d of the base (or of the emitter) is large compared to the diffusion length L of the minority carriers, J_d can be written [2]

$$J_d = q \int_{\lambda_1}^{\lambda_2} \frac{\phi(\lambda)\alpha(\lambda)L}{1+\alpha(\lambda)L} \exp[-\alpha(\lambda)(d+W)]\,d\lambda \tag{5}$$

where $\phi(\lambda)$ is the illumination flux at the wavelength λ, extending from λ_1 to λ_2, and $\alpha(\lambda)$ is the absorption coefficient of the material at λ (λ_2 corresponds to the limit of absorption, i.e. to the gap of the material, while λ_1 is the lowest wavelength for which $\phi(\lambda)$ is non-negligible). Such a current is non-negligible when $\alpha(\lambda)(d+W)$ is small, in which case the term

$$C = \exp[-\alpha(\lambda)(d+W)] \tag{6}$$

is of the order of 1. For the solar spectrum the product $C(\lambda)\phi(\lambda)$ is then a slowly varying function in the (λ_1, λ_2) range. The amplitude variation of this product is at most 50% of its maximum (see figure 2). Hence this variation is small compared to that of $\alpha(\lambda)$ which, for λ values lower than λ_2, for Si and GaAs, can be reasonably well approximated by an exponential function [3]

$$\alpha(\lambda) = \alpha(0)\exp(-r\lambda). \tag{7}$$

As a result the product $C(\lambda)\phi(\lambda)$ can be considered as a constant, A, and J_d becomes

$$J_d = qA \int_{\lambda_1}^{\lambda_2} \frac{\alpha(\lambda)L}{1+\alpha(\lambda)L}\,d\lambda. \tag{8}$$

Differentiation of this expression

$$d\alpha(\lambda) = -r\alpha(\lambda)\,d\lambda \tag{9}$$

allows one to write

$$d\lambda = \frac{-1}{r}\frac{d\alpha(\lambda)}{\alpha(\lambda)}. \tag{10}$$

Then, expression (8) can be transformed into

$$J_d = \frac{qA}{r}\int_{\alpha(\lambda_2)}^{\alpha(\lambda_1)} \frac{d[L\alpha(\lambda)]}{1+L\alpha(\lambda)} \tag{11}$$

which can be then integrated

$$J_d = \frac{qA}{r}\left[\ln\left(\alpha(\lambda_1)+L^{-1}\right) - \ln\left(\alpha(\lambda_2)+L^{-1}\right)\right]. \tag{12}$$

For $\lambda > \lambda_1$, we have $\alpha(\lambda_1) \gg \alpha(\lambda_2)$ in usual cases. Moreover $\alpha(\lambda_1)$ is larger than L^{-1}, which is not the case for $\alpha(\lambda_2)$. Then J_d reduces to

$$J_d = \frac{qA}{r}\ln\left[\frac{\alpha(\lambda_1)}{\alpha(\lambda_2)+L^{-1}}\right]. \tag{13}$$

It is only when the irradiation has severely decreased L, that L^{-1} becomes larger than $\alpha(\lambda_2)$, in which case J_d can be approximated by

$$J_d = \frac{qA}{r}\left[\ln\alpha(\lambda_1) - \ln(L^{-1})\right]. \tag{14}$$

The diffusion length L is defined as

$$L^2 = D\tau \tag{15}$$

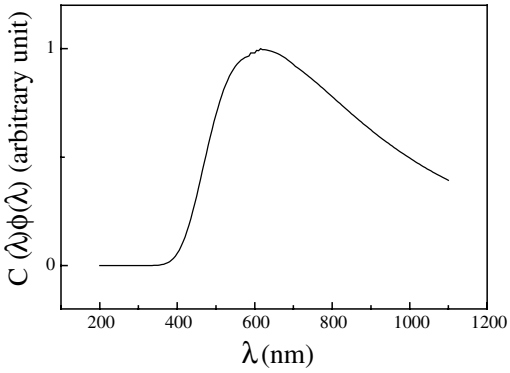

Figure 2. Normalized variation of the product $C(\lambda)\phi(\lambda)$ for a Si cell.

where D is the diffusion coefficient of the minority carriers and

$$\tau = (N\sigma v)^{-1} \tag{16}$$

the lifetime. In this last expression N is the concentration of the recombination centres, σ is their capture cross section for minority carriers and v is the thermal velocity. Introducing these notations in expression (14) leads to

$$J_{\mathrm{d}} = \frac{qA}{r}\left[\ln\alpha(\lambda_1) - \ln\left(\frac{N\sigma v}{D}\right)^{1/2}\right]. \tag{17}$$

The recombination centres being introduced by the irradiation with a rate k

$$N = k\varphi \tag{18}$$

we arrive at the result

$$J_{\mathrm{d}} = \frac{qA}{r}\left[\ln\alpha(\lambda_1) - \ln\left(\frac{k\sigma v}{D}\right)^{1/2} - \frac{1}{2}\ln\varphi\right] \tag{19}$$

which shows that J_{d} decreases linearly with $\ln\varphi$, i.e. one can write

$$J_{\mathrm{d}} = \xi - \rho\log\varphi. \tag{20}$$

The slope ρ of the plot J_{d} versus $\log\varphi$

$$\rho = 2.3\frac{qA}{2r} \tag{21}$$

is independent of the recombination centres introduced by the irradiation. It depends only on the illumination conditions, through A, and on the material, through the constant r characterizing the absorption coefficient. It is the value ξ of J_{d} at the origin ($\log\varphi = 0$) which contains the characteristics of the recombination centre

$$\xi = \frac{qA}{r}\left[\ln\alpha(\lambda_1) - \frac{1}{2}\ln\left(\frac{k\sigma v}{D}\right)\right]. \tag{22}$$

This result demonstrates that photovoltaic cells made of the same material exhibit identical slopes for the degradation, even if the recombination centres introduced by the irradiation are different. This is well illustrated in figure 3 which presents the same data as in figure 1, showing that the slopes of degradation are identical for different Si cell types (a–c). The nature and concentration of these centres are given by the value ξ of J_{d} extrapolated at the origin.

Degradation of J_{SC} occurs for a fluence larger than a minimum fluence φ_{m} for which

$$\xi - \rho\log\varphi_{\mathrm{m}} = J_{\mathrm{SC}}(0) \tag{23}$$

where $J_{\mathrm{SC}}(0)$ is the value prior to irradiation. This minimum fluence, given by

$$\log\varphi_{\mathrm{m}} = \frac{\xi - J_{\mathrm{SC}}(0)}{\rho} \tag{24}$$

is therefore related to the irradiation-induced recombination centres, through ξ, and to the native recombination centres, through $J_{\mathrm{SC}}(0)$.

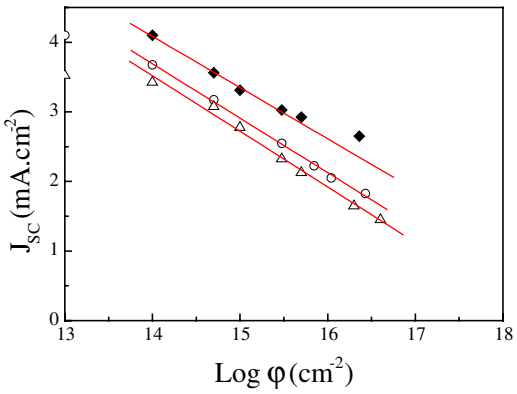

Figure 3. Variations of the short-circuit current versus fluence for the type a (♦), b (○) and c (△) Si cells. The data are those of figure 1.

2.2. *Open-circuit voltage*

The forward current density in the dark of a junction is the sum of a diffusion current and of recombination current densities

$$J(V) = J_1\left[\exp\left(\frac{qV}{kT}\right) - 1\right] + J_2\left[\exp\left(\frac{qV}{2kT}\right) - 1\right] \tag{25}$$

where J_1 and J_2 are given by the following expressions (see, for instance, in [4] and recently in [5]):

$$J_1 = \frac{qn_{\mathrm{i}}^2\sqrt{D_{\mathrm{n}}}}{N_{\mathrm{A}}\sqrt{\tau_{\mathrm{n}}}} + \frac{qn_{\mathrm{i}}^2\sqrt{D_{\mathrm{h}}}}{N_{\mathrm{D}}\sqrt{\tau_{\mathrm{h}}}} \tag{26}$$

and

$$J_2 = \frac{\pi}{2}\frac{n_{\mathrm{i}}kT}{\sqrt{\tau_{\mathrm{n}}\tau_{\mathrm{h}}}}\frac{W_0}{\sqrt{V_{\mathrm{d}}}}. \tag{27}$$

In these expressions n_{i} is the intrinsic carrier concentration, $D_{\mathrm{n,h}}$ are the electron, hole diffusion coefficients, $\tau_{\mathrm{n,h}}$ are the minority carrier lifetime in the p, n regions, $N_{\mathrm{A,D}}$ are the acceptor, donor doping on each side of the junction, V_{d} is the built-in voltage and W_0 is the width of the space charge region with no applied bias.

Using expressions (15) and (16) and introducing the rate k given by (18), we can rewrite the above two expressions in the following way:

$$J_1 = J_1^*\,\varphi^{1/2} \tag{28}$$

$$J_2 = J_2^*\,\varphi \tag{29}$$

with

$$J_1^* = qn_{\mathrm{i}}^2\left[\left(\frac{k\sigma_{\mathrm{n}}v_{\mathrm{n}}D_{\mathrm{n}}}{N_{\mathrm{A}}}\right)^{1/2} + \left(\frac{k\sigma_{\mathrm{h}}v_{\mathrm{h}}D_{\mathrm{h}}}{N_{\mathrm{D}}}\right)^{1/2}\right] \tag{30}$$

and

$$J_2^* = \frac{\pi}{2}n_{\mathrm{i}}kT\,W_0\left(\frac{k^2\sigma_{\mathrm{n}}\sigma_{\mathrm{h}}v_{\mathrm{n}}v_{\mathrm{h}}}{V_{\mathrm{d}}}\right)^{1/2}. \tag{31}$$

Hence, according to expression (4) we have

$$J_{\mathrm{SC}} = J_1^*\,\varphi^{1/2}\exp\left(\frac{qV_{\mathrm{OC}}}{kT}\right) \tag{32}$$

in case the dark current is essentially induced by the diffusion regime. In case it is mostly due to the recombination regime

$$J_{\mathrm{SC}} = J_2^*\,\varphi\exp\left(\frac{qV_{\mathrm{OC}}}{2kT}\right). \tag{33}$$

Thus, in both cases, V_{OC} can be written under the form

$$V_{OC} = \varepsilon - \eta \log \varphi \tag{34}$$

where the slope η of the plot V_{OC} $(\log \varphi)$

$$\eta = 2.3/2\frac{kT}{q} \qquad \text{for a diffusion regime} \tag{35}$$

and

$$\eta = 2.3\frac{2kT}{q} \qquad \text{for a recombination regime} \tag{36}$$

takes the values 3×10^{-2} and 1.2×10^{-1} (φ in cm^{-2}) at 300 K for diffusion and recombination regimes, respectively.

The value of V_{OC} at the origin ($\log \varphi = 0$)

$$\varepsilon = \frac{kT}{q} \ln\left(\frac{J_{SC}}{J_1^*}\right) \qquad \text{for a diffusion regime} \tag{37}$$

or

$$\varepsilon = \frac{2kT}{q} \ln\left(\frac{J_{SC}}{J_2^*}\right) \qquad \text{for a recombination regime} \tag{38}$$

thus provides J_1^* and J_2^*, from which information on the recombination centre can be extracted using expressions (30) and (31).

3. Experimental results

The solar cells studied are n$^+$/p Si, p$^+$/n GaAs and n$^+$/p GaInP cells. The Si cells are either Czochralski (Cz) grown or MOCVD epitaxially (epi) grown with dopings in the range 1–10 Ω cm. They are referred to in the text as: type a (Cz, 10 Ω cm); type b (Cz, 2 Ω cm); type c (epi, 10 Ω cm); and type d (epi, 1 Ω cm). The GaAs cells are all MOCVD epitaxially grown with bases doped at a level between 1 and 3×10^{17} cm^{-3}. The GaInP cells, also MOCVD grown, have a base doped at a level of 1.5×10^{17} cm^{-3}.

These cells have been irradiated with increasing fluences, in the range 10^{14} to 10^{17} electrons cm^{-2}, at an energy of 1 MeV. The irradiation was performed at room temperature with a scanned beam in order to ensure the uniformity of the fluence over the area of the cell (1–4 cm^2). The intensity of the beam (2 μA) was chosen to keep negligible the temperature increase. The cells are placed in a Faraday cup allowing accurate measurement of the fluence with a current integrator. Current–voltage measurements were performed *in situ* in the accelerator under a 0.1 AMO illumination provided by a Xe arc lamp.

The variations of the short-circuit currents and open-circuit voltages versus fluence of these cells are given in figures 3, 4, 5 and 6, respectively. Note that in all the figures the values of $J_{SC}(0)$ or $V_{OC}(0)$ are those indicated for the lowest fluence.

4. Analysis of the data

4.1. Open-circuit voltage degradation

4.1.1. GaAs cells. Degradation occurs for $\log \varphi_m > 14.6$ (electrons cm^{-2}) and is characterized by $\eta = 0.11$ V $(\log \varphi)^{-1}$ and $\varepsilon = 0.87$ V. The value of η is the value we expect for a regime recombination (see section 2.2).

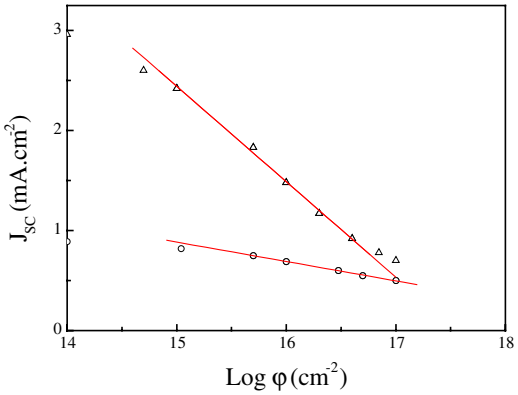

Figure 4. Variation of the short-circuit current versus fluence for GaAs (△) and GaInP (○) cells.

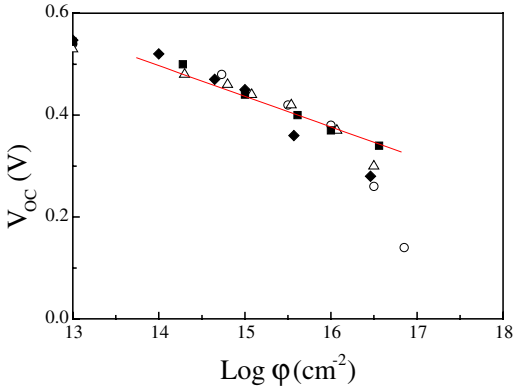

Figure 5. Variations of the open-circuit voltage versus fluence for the type a (♦), b (○), c (△) and d (■) Si cells.

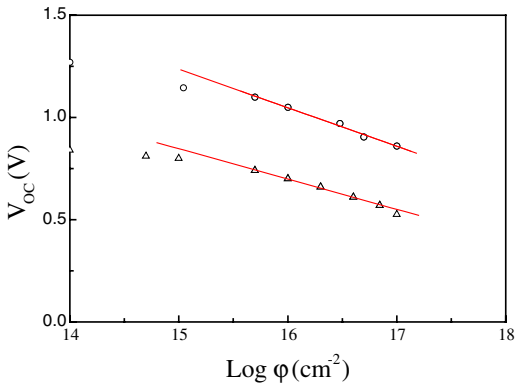

Figure 6. Variation of the open-circuit voltage versus fluence for GaAs (△) and GaInP (○) cells.

4.1.2. GaInP cells. In this case: $\eta = 0.11$ V $(\log \varphi)^{-1}$ and $\varepsilon = 1.25$ V. The degradation is already observed for the lowest fluence ($\log \varphi = 14$), so that $V_{OC}(0) = \varepsilon$. Again η fits the expected value for a recombination regime.

4.1.3. Si cells. For the Si cells a common behaviour $\eta = 6 \times 10^{-2}$ V $(\log \varphi)^{-1}$ is observed, in the full range of $\log \varphi$ values for the type c and d (epi) cells and only below $\log \varphi = 16$ (electrons cm^{-2}) for the type b cell. For the type a cell, an additional behaviour is observed for $\log \varphi$ larger than 15 (electrons cm^{-2}) for which $\eta = 0.11$ V $(\log \varphi)^{-1}$, which must

Table 1. Experimental values of the different parameters from which the quantity $k^2\sigma_n\sigma_h$ (product of the introduction rate and of the electron and hole capture cross sections) is deduced.

Cell	J_2^* (A cm^{-2} φ^{-1})	J_2'' (A cm^{-2} φ^{-1})	η (V log φ^{-1})	ε (V)	$k^2\sigma_n\sigma_h$ (cm^2)
GaAs	2.1×10^{-25}	–	1.1×10^{-1}	2.54	1.5×10^{-26}
GaInP	1.3×10^{-28}	–	1.1×10^{-1}	2.89	1.9×10^{-22}
Si (a)	5.7×10^{-22}	–	1.1×10^{-1}	2.20	9.0×10^{-29}
Si (a)	–	7.8×10^{-25}	6.0×10^{-2}	1.33	6.5×10^{-27}
Si (b)	–	1.0×10^{-24}	6.0×10^{-2}	1.32	1.0×10^{-23}
Si (c)	–	4.0×10^{-25}	6.0×10^{-2}	1.34	1.7×10^{-27}
Si (d)	–	8.2×10^{-25}	6.0×10^{-2}	1.32	1.4×10^{-25}

Table 2. Experimental values of the different parameters from which the product $k\sigma_{n,h}$ (product of the introduction rate times the minority carrier capture cross section) is deduced. The data correspond to an illumination of 0.1 AMO.

Cell	$J_{SC}(0)$ (mA cm^{-2})	ρ (mA cm^{-2} log φ^{-1})	$\alpha(\lambda_2) + L_0^{-1}$ (cm^{-1})	$k\sigma_{n,h}$ (cm)
Si (a)	4.6	0.87	22	4.3×10^{-17}
Si (b)	4.1	0.87	42	1.1×10^{-16}
Si (c)	3.5	0.87	–	4.3×10^{-17}
Si (d)	3.5	0.87	–	1.8×10^{-16}
GaAs	3.0	1.00	5.0×10^3	3.1×10^{-13}
GaInP	0.9	0.19	7.5×10^3	1.7×10^{-13}

therefore be ascribed to a recombination regime. The first behaviour, although characterized by a different value of η, is also associated with a recombination regime. The reason the value of η is different is the following: the ideality factor n of the junction, once irradiated, is no longer equal to 2 and expression (33) must be replaced by

$$I_{SC} = J_2'' \varphi \exp\left(\frac{q V_{OC}}{nkT}\right). \tag{39}$$

The linear dependence of V_{OC} versus $\log \varphi$ given by expression (34) remains valid, but η is no longer equal to 0.11 V $(\log \varphi)^{-1}$; its value is: $5.8 \times 10^{-2} n$ V $(\log \varphi)^{-1}$. The experimental value we measured therefore corresponds to $n = 1.05$. The physical origin of this n value lies in the fact that the current corresponding to the Shockley–Read recombination is not exactly that indicated in expression (25), but is modulated by a factor depending on the location of the energy level E_t associated with the recombination centre compared to the intrinsic Fermi level E_{Fi}, so that $\frac{\pi}{2}$ in expression (27) of J_2^* must be replaced by $(\mathrm{ch}\, x)^{-1}$, where x is the quantity (see, for instance, [4])

$$x = \frac{E_t - E_{Fi}}{kT} + \frac{1}{2} \ln\left(\frac{\tau_h}{\tau_n}\right). \tag{40}$$

When the capture times of the electrons and holes, τ_n and τ_h, on the recombination centre are equivalent, the magnitude of n corresponds to the presence of a defect located at 0.3 eV above the valence band (the value of x is of the order of 9).

Finally, from the value of ε and knowing J_{SC} (see below), we deduce J_2^* from expression (31), associated with the recombination regime by application of expression (38). Once J_2^* is determined, we get $k^2\sigma_n\sigma_h$ from expression (31). The results are given in table 1.

4.2. Short-circuit current degradation

The linear dependence of J_{SC} versus $\log \varphi$ is observed for all the cells. It is limited to a maximum fluence, either because the diffusion current becomes too small (this is the case of the highly doped GaAs cell) or because trapping centres have compensated the doping impurities, destroying the junction.

The observation confirms the theory. First, the slope ρ depends only on the conditions of illumination and is the same for a given material (Si), whatever the doping and growth mode (see figure 3). We observe that, with the same illumination, ρ is larger for a GaAs cell than for a Si cell: this is due to the fact that r is larger in GaAs than in Si. The ratios of the ρ and r values are the same, confirming that ρ is only a function of r when the illumination is kept constant. The initial values of the short-circuit current $J_{SC}(0)$ are given in table 2, together with the experimental values of the slopes ρ.

The knowledge of ρ and ξ allows one to calculate the product $k\sigma$ of the recombination centre by replacing $\frac{A}{r}$ in equation (22) by its expression (21) in terms of ρ. Introducing the fluence φ_f for which $I_{SC} = 0$, which can be determined by the extrapolation of the experimental results, we extract $k\sigma$ from

$$J_{SC}(0) - \rho \log \varphi_f = \frac{2\rho}{2.3}\left[\frac{1}{2} \ln\left(\frac{k\sigma V}{D}\right) - \ln\left(\alpha(\lambda_2) + L_0^{-1}\right)\right] \tag{41}$$

assuming L_0^{-1}, the inverse of the initial diffusion length, is small compared to the lowest value of the absorption coefficient $\alpha(\lambda_2)$. For the GaAs and GaInP cells, $\alpha(\lambda_2)$ is very large (5 and 7×10^3 cm^{-1}, respectively) and the approximation $\alpha(\lambda_2) \gg L_0^{-1}$ is verified, even when the initial lifetime is small. The determination of the product $k\sigma$ is then more accurate for GaAs and GaInP than for Si.

As an illustration, consider the case of the type a Si cell, for which $J_{SC}(0) = 4.6$ mA cm^{-2} and $\rho = 0.87$ mA cm^2 $(\log \varphi)^{-1}$. We determine graphically on the experimental plot $J_{SC}(\log \varphi)$: $\varphi_f = 6.4 \times 10^{18}$ cm^{-2} and from figure 3 $\alpha(\lambda_2) = 20\,\mathrm{cm}^{-1}$. Using (41), we calculate $J_{SC}(0) - \rho \log \varphi_f = -9$ mA and obtain $k\sigma = 4.2 \times 10^{-17}$ cm (with $D = 32$ cm^2 s^{-1} and

$v = 1.1 \times 10^7 \text{cm s}^{-1}$). The $k\sigma$ values obtained for the other cells are given in table 2.

5. The nature and characteristics of the recombination centres

5.1. Introduction

A recombination centre is characterized by its concentration N (or introduction rate k), its ionization energy E_t and the electron and hole capture cross sections, σ_n and σ_h. In order to obtain these four parameters one should have four independent relationships containing one or several of these parameters. The fluence dependence of V_{OC} and J_{SC} provides two relations: $k\sigma_n$ (or $k\sigma_h$) and $k^2\sigma_n\ \sigma_h$. The two others can be obtained from DLTS and from the study of the J–V characteristics in the dark. Defect spectroscopy provides the concentration, energy level and the capture cross section for majority carriers, provided the corresponding defect can be recognized as being a recombination centre. But, when using DLTS, all the detected defects are in a situation where they behave as majority carrier traps. Hence, it is not possible to sort out which of the detected defects is a recombination centre. However, because a non-radiative recombination centre is expected to lie in the middle of the gap, we can compare the magnitude of the cross sections of the deepest traps with that obtained by the other techniques, directly sensitive to recombination centres, in order to recognize it.

The J–V characteristics in the dark, plotted as $\log J(V)$, exhibits two behaviours (see equation (25)): in the low-bias range, the so-called Shockley–Read recombination regime dominates, which is recognized by the linear dependence of $\log J$ versus V with a slope $\frac{q}{2kT}$. In this regime the extrapolation of $\log I$ to $V = 0$ provides the recombination current J_2 whose expression (see (27)), contains $\tau_{n,h}$, related to N and $\sigma_{n,h}$, giving a new relationship between N and $\sigma_{n,h}$. In the high-bias range the diffusion regime, for which the slope of the $\log J$ versus V is $\frac{q}{kT}$, dominates. In this case, we can evaluate the current J_1 given by expression (26), containing $\tau_{n,h}$. In practice, one of the two terms in this expression is negligible in front of the other and J_1 gives a fourth relationship between N and σ_n or σ_h.

In the next section we use these considerations, by taking advantage of previous works on the characterization of electron-induced defects in Si, GaAs and GaInP by DLTS and by, eventually, acquiring new data concerning J–V characteristics in the dark.

5.2. Defects in GaAs

Defects induced by electron irradiation in n- and p-type materials have been extensively studied (for a review see [6]). These studies demonstrated that the defects introduced by room-temperature irradiation are primary defects, resulting from the displacements of As in the As sublattice [7]. Their characteristics deduced from DLTS data are summarized in tables 3 and 4. E_4, E_5 and H_3 are deep in the gap and could be ascribed to a recombination centre. For all these defects, k is of the order of 0.1 cm^{-1}. From the analysis of J_{SC} and V_{OC}, we obtained $k^2\sigma_n\sigma_h = 4 \times 10^{-27}\ \text{cm}^{-2}$ and $k\sigma_n = 3.1 \times 10^{-13}$ cm (see tables 1 and 2). The value of $k^2\sigma_n\sigma_h$ is confirmed by the $\log J(V)$ characteristics in the dark (see table 5), which exhibit only the recombination regime (see figure 7). We therefore deduce $k\sigma_h = 1.3 \times 10^{-14}$ cm and, using $k = 0.1\ \text{cm}^{-1}$, we get $\sigma_n = 3.1 \times 10^{-12}\ \text{cm}^2$ and $\sigma_h = 1.3 \times 10^{-13}\ \text{cm}^2$. These values seem to correspond to the electron trap E_5 and to the hole trap H_3. Taking the exact values of k for each of these traps, we finally get $\sigma_n = 3.9 \times 10^{-12}\ \text{cm}^2$ and $\sigma_h = 6 \times 10^{-14}\ \text{cm}^2$. These two traps characterized by ionization energies of 0.96 and 0.71 eV respectively, could in fact correspond to the same

Table 3. Characteristics of the electron traps induced in GaAs by electron irradiation obtained by DLTS (E_C is the bottom of the conduction band).

Defects	$k\,(\text{cm}^{-1})$	$E_C - E_t$ (eV)	$\sigma_n\,(\text{cm}^2)$
E_1	1.50	0.045	2.2×10^{-15}
E_2	1.50	0.140	1.2×10^{-13}
E_3	0.40	0.300	6.2×10^{-15}
E_4	0.08	0.760	3.1×10^{-14}
E_5	0.10	0.960	1.9×10^{-12}

Table 4. Characteristics of the hole traps induced in GaAs by electron irradiation obtained by DLTS (E_V is the top of the valence band).

Defects	$k\,(\text{cm}^{-1})$	$E_V + E_t$ (eV)	$\sigma_h\,(\text{cm}^2)$
H_0	0.8	0.06	1.6×10^{-16}
H_1	0.1–0.7	0.29	5.0×10^{-15}
H_2	–	0.41	2.0×10^{-16}
H_3	0.2	0.71	1.2×10^{-14}

Table 5. Values of the parameters deduced for the recombination and diffusion currents extracted from the current–voltage characteristics in the dark. The experimental data from which these parameters are extracted are not presented, except for the case of GaAs (figure 7).

Cell	Diffusion $k\bar{\sigma}_n$ (cm)	Recombination $k^2\sigma_n\sigma_h$ (cm^2) ($b > 1$)	Recombination $k^2\sigma_n\sigma_h$ (cm^2) ($b < 1$)
Si (a)	5.6×10^{-17}	–	4.9×10^{-29}
Si (b)	5.6×10^{-16}	–	–
Si (c)	3.2×10^{-16}	3.7×10^{-29}	–
Si (d)	5.6×10^{-17}	7.5×10^{-28}	–
GaAs	–	–	4.0×10^{-27}
GaInP	–	–	1.2×10^{-23}

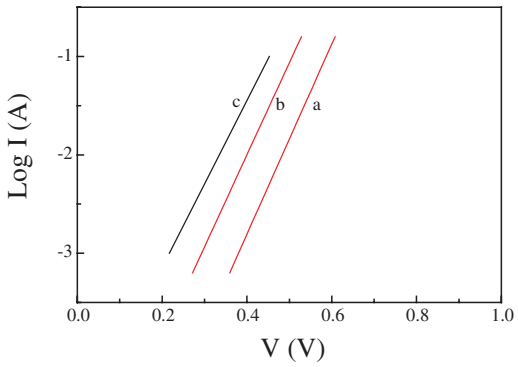

Figure 7. Current–voltage characteristics in the dark of the GaAs cell for different fluences: 1×10^{15} (a), 1×10^{16} (b), 5×10^{16} (c) cm^{-2} monitored at room temperature. The slopes of these plots are equal to $q/2kT$.

centre because the electron–phonon interaction is expected to be large, in such a way that their energy levels are smaller than their ionization energy.

We therefore conclude that the non-radiative recombination centre induced by electron irradiation in GaAs is a primary defect, most probably related to a particular configuration of the As vacancy–interstitial pair [8, 9], corresponding to the E_5 electron trap and the H_2 hole trap. Its characteristics are $k \approx 0.1\,\mathrm{cm}^{-1}$, $\sigma_n = 4 \times 10^{-12}$ and $\sigma_h = 6 \times 10^{-14}\,\mathrm{cm}^2$.

5.3. Defects in InGaP

There has been only one study of the defects introduced by electron irradiation in n-type InGaP [10]. However, recently a systematic programme on electron-induced defects has been performed on n^+/p structures [11–14]. Two hole traps and three electron traps were detected. It has been clearly demonstrated, by a direct comparison between the annealing behaviour of the H_2 trap and the photovoltaic properties of a solar cell, that this trap is the main recombination centre [13]. For this centre $k = 9.3 \times 10^{-2}\,\mathrm{cm}^{-1}$. From table 1, we have $k^2\sigma_n\sigma_h = 1.9 \times 10^{-22}\,\mathrm{cm}^2$ (we select the value given by the analysis of J_{SC}, the one provided by the analysis of V_{OC} being less accurate); from table 2 we have $k\sigma_n = 1.7 \times 10^{-13}\,\mathrm{cm}^2$.

We therefore deduce that the recombination centre is the H_2 trap characterized by $k = 0.9 \times 10^{-1}\,\mathrm{cm}^{-1}$, $\sigma_n = 1.8 \times 10^{-12}\,\mathrm{cm}^2$, $\sigma_h = 1.2 \times 10^{-8}\,\mathrm{cm}^2$. As we shall develop in a further work this defect is apparently complex involving a primary defect and the doping impurity (Zn). Hence, the value of k depends on the doping concentration and the value we report here is only correct in the case considered.

5.4. Defects in Si

In Si, the defects introduced by electron irradiation have been identified using mainly DLTS and paramagnetic resonance (for a tutorial review on this question see [14]). These defects, when created at room temperature are, in majority, complexes of the mobile vacancy with the dominant impurities: (O in Cz materials), the doping impurity and with themselves, which are commonly labelled the A centre, E centre and the divacancy, respectively. However, the defects which are non-radiative recombination centres, have not been identified among all the detected defects.

The $k\sigma_n$ values given in table 2 are coherent with that provided by the analysis of the diffusion current in the dark, made from data extracted for $J(V)$ characteristics in the dark given in table 5; they are also coherent with the $k^2\sigma_n\sigma_h$ value of table 1. Some of these characteristics exhibit two slopes because of the presence of two recombination centres, one of which is associated with an energy level close to the valence band. In this last case a parameter b must be included in the recombination current [4] which is characteristic of this energy level.

The analysis of V_{OC} has shown that there is a common recombination centre, which we label X, in the epi and Cz materials. Only in the type a cell is there an additional centre, labelled Y. We have shown in section 4.1.3. that the X centre is characterized by an energy level at 0.3 eV above the valence band. For this level, we notice that the ratio of the parameter $k^2\sigma_n\sigma_h$ for the type c and d cells has a value (20.2) nearly equal to the square of the $k\sigma$ ratio (17.9). Because the σ_n, σ_h values should be common for all cells, the origin of this behaviour should be in the doping dependence of the introduction rate k. This implies that the X centre is associated with a defect involving the doping impurity.

We shall demonstrate, in a work treating the compensating centres introduced by irradiation, that such centres are characterized by a doping dependence of the introduction rate identical to the one we observe here. We show that this dependence is expected for a defect produced by the interaction of mobile primary defects with the p-type doping impurities. We can therefore conclude that the X centre is the so-called E centre, i.e. the vacancy complexed with the doping impurity (B in this case). This assignment is in agreement with DLTS studies which have identified this defect and demonstrated that its associated energy level lies at 0.27 eV above the valence band. From the dependence of k versus the doping concentration and using the values of $k^2\sigma_n\sigma_h$ given in tables 1 and 2, we evaluate the capture cross section: $\sigma_n \approx 10^{-15}\,\mathrm{cm}^2$ and $\sigma_h \approx 10^{-11}\,\mathrm{cm}^2$.

Concerning the second recombination centre, Y, only detected in the type a cell, the only information we have been able to extract is $k^2\sigma_n\sigma_h = 9 \times 10^{-29}\,\mathrm{cm}^2$, and we know that its energy level should be located near the midgap. Since this centre is not observed in the Cz cells, it cannot be related to the presence of oxygen. Since it is observed in a low-doped Cz (type a cell) material and not in a more doped one (type b cell), and is not directly related to the doping impurity, we suggest that it must be related to the divacancy (which is associated with an energy level at 0.39 eV below the conduction band). Indeed, divacancies are formed by mobile interacting vacancies; their concentration is large only when the mobile vacancies are not first trapped by O impurities or the dopants. Taking $\sigma_n \approx 10^{-15}\,\mathrm{cm}^2$ for the $E_C - 0.39$ eV level of the divacancy, we get $\sigma_h \approx 10^{-10}\,\mathrm{cm}^2$ if we assume $k \approx 3 \times 10^{-2}\,\mathrm{cm}^{-1}$. This value of σ_h is obviously too large, and our evaluation of k is probably incorrect. As explained in [15], the introduction rates of the divacancy, as well as that of the E centre, depend strongly on the doping and oxygen concentrations.

6. Conclusion

We have performed a detailed analysis of the dependence, versus the logarithm of the irradiation fluence φ, of the short-circuit current I_{SC} and of the open voltage V_{OC} of a solar cell. We have determined the conditions in which these quantities vary linearly with $\log \varphi$. We show that the slopes of these plots are independent of the nature and concentration of the recombination centres introduced by the irradiation and depend only on the illumination conditions and on the absorption coefficient of the material which composes the solar cell. We explain how information concerning these centres can be extracted from these plots.

We then correlate the above information with others derived from DLTS and current–voltage characteristics in the dark to determine the concentrations and electron and hole capture cross sections of the recombination centres. This procedure has been applied to Si, GaAs and InGaP solar cells

to obtain the characteristics of the recombination centres in these materials and to identify them.

Acknowledgments

We thank G Strobl (Tessag-ASE, Germany), P Iles (Tecstar, USA), S Taylor (EEV-Marconi, UK) and M Yamaguchi (Toyota Institute, Japan) for kindly providing the solar cells used in this study. This work has been partly supported by a Tessag-ASE contract.

References

[1] Bourgoin J C and de Angelis N 2001 *Sol. Energy Mater. Sol. Cells* **66** 467
[2] Hovel H J 1979 *Semiconductors and Semimetals* vol 11 (New York: Academic)
[3] Dash W C and Newman R 1951 *Phys. Rev.* **99** 1151
Hill D E 1964 *Phys. Rev.* **133** A866
[4] Shockley W 1957 *Proc. IRE* **50** 1228
[5] Simoen E, Vantellmont J and Layes C 1996 *Appl. Phys. Lett.* **69** 2858
[6] Pons D and Bourgoin J C 1985 *Solid State Phys.* **18** 3839
[7] Stievenard D, Boddaert X and Bourgoin J C 1986 *Phys. Rev.* B **34** 4048
[8] Lim H J, Von Barbelaben H J and Bourgoin J C 1987 *J. Appl. Phys.* **62** 2738
[9] Stievenard D, Boddaert X, Bourgoin J C and Von Barbelaben H J 1990 *Phys. Rev.* B **41** 5271
[10] Zaidi M A, Zazoui M and Bourgoin J C 1993 *J. Appl. Phys.* **73** 7229
[11] Kahn A, Yamaguchi M, Takamoto T, De Angelis N and Bourgoin J C 2000 *J. Cryst. Growth* **210** 264
[12] Kahn A, Yamaguchi M, Bourgoin J C, Ando K and Takamoto T 2001 *J. Appl. Phys.* **89** 4263
[13] Kahn A, Yamaguchi M, Bourgoin J C, de Angelis N and Takamoto T 2000 *Appl. Phys. Lett.* **76** 2559
[14] De Angelis N, Bourgoin J C, Takamoto T, Kahn A and Yamaguchi M 2001 *Sol. Energy Mater. Sol. Cells* **66** 495
[15] Bourgoin J C and Lannoo M 1983 *Point Defects in Semiconductors* vol 2 (Berlin: Springer) ch 8